Supplementary Information

Water-soluble, nitrogen-doped fluorescent carbon dots for highly sensitive and selective detection of Hg^{2+} in aqueous solution

Y. Zhang[a,b], Y. H. He[a,c], P. P. Cui[e], X. T. Feng[a,c], L. Chen[a,c], Y. Z. Yang*[c,d] and X. G. Liu*[a,c]

[a] *College of Chemistry and Chemical Engineering, Taiyuan University of Technology, Taiyuan 030024, China*

[b] *Department of Chemistry and Chemical Engineering, Lyuliang University, Lyuliang 033001, China*

[c] *Key Laboratory of Interface Science and Engineering in Advanced Materials (Taiyuan University of Technology), Ministry of Education, Taiyuan 030024, China*

[d] *Research Center on Advanced Materials Science and Technology, Taiyuan University of Technology, Taiyuan 030024, China*

[e] *College of Materials Science and Engineering, Taiyuan University of Technology, Taiyuan 030024, China*

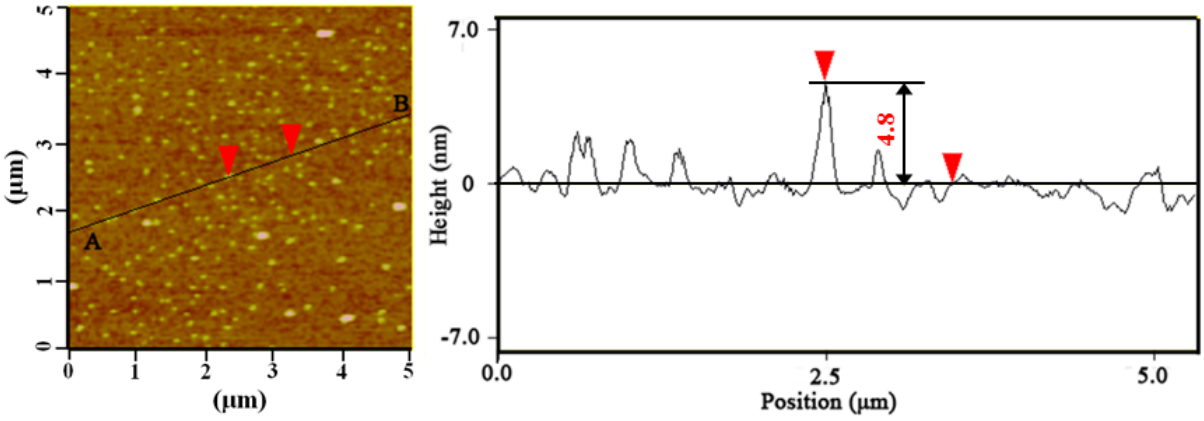

Fig. S1. AFM topography image of NCDs on silicon substrate with height profile along line AB in the image.

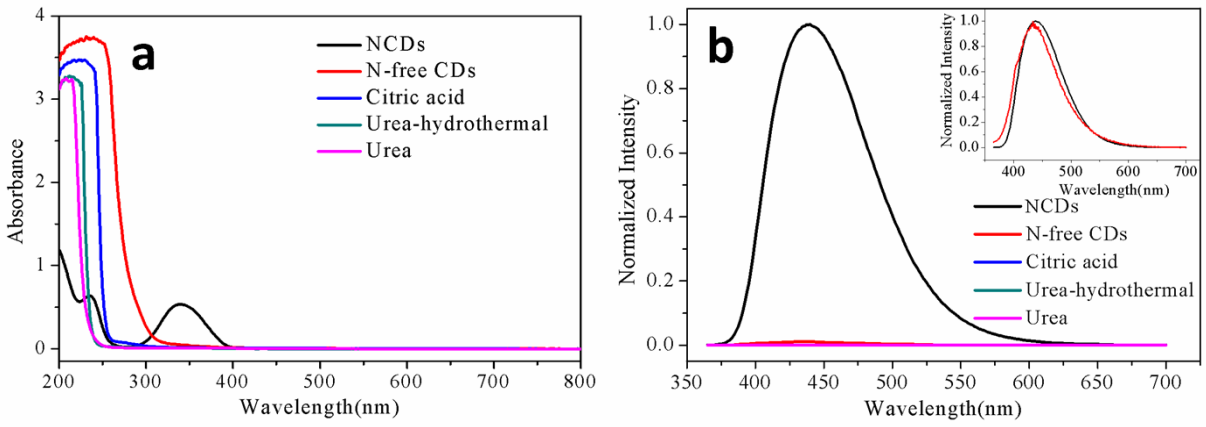

Fig. S2. UV-vis absorption (a) and PL spectra (b) of NCDs, N-free CDs, Citric acid, Urea-hydrothermal and Urea. Inset of (b) shows normalized PL spectra of NCDs and N-free CDs (Citric acid: 4.2 g citric acid+40 mL H_2O; Urea: 3.6 g urea+40 mL H_2O; N-free CDs: 4.2 g citric acid+40 mL H_2O, 180℃, 4h; Urea-hydrothermal: 3.6 g urea+40 mL H_2O, 180℃, 4h; NCDs: 4.2 g citric acid + 40 mL H_2O + 3.6 g urea, 180℃, 4h. The concentration of NCDs is diluted to 2×10^{-4} times that of the original solution. The excitation and emission slits are both set at 2 nm, λ_{ex}= 355 nm).

QY measurements

The QY of CDs was determined by slope method (Fig. S2). Quinine sulfate (literature QY=0.54 at 360 nm) in 0.1 M H_2SO_4 (n=1.33) was chosen as the standard reference sample to calculate the QY of CDs in water (n=1.33). All the absorbance values (keeping less than 0.1 at 360 nm in order to minimize reabsorption) of the solutions were recorded on UV-vis spectrophotometer. PL spectra (excited at 360 nm) of all sample solutions were measured on spectrometer. Integrated fluorescence intensity is the area under the PL curve in the wavelength range from 370 to 700 nm. Then, a graph was plotted using the integrated fluorescence intensity against the absorbance and a trend line was added for each curve with intercept at zero. Then QY of CDs was calculated according to the equation:

$$\mathbf{Q_x = Q_{st}\,(Grad_x/Grad_{st})(\eta_x/\eta_{st})^2}$$

where Q is the QY, Grad is the gradient from the plot of integrated fluorescence intensity versus absorbance and η is the refractive index of the solvent. The subscript "st" refers to the quinine sulfate and "x" refers to CDs. For these aqueous solutions, η_x/η_{st}=1.

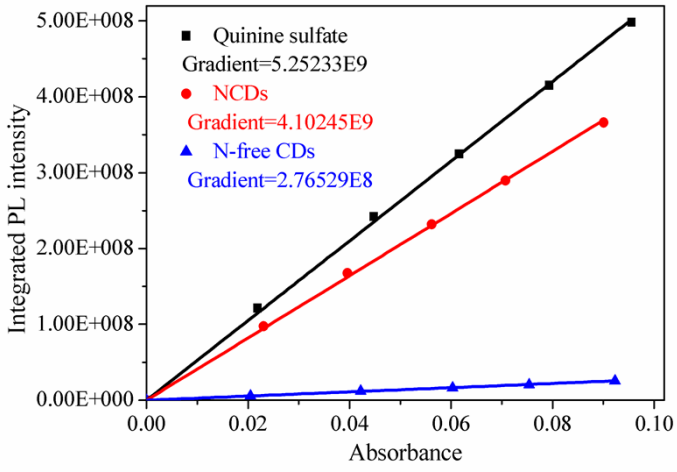

Fig. S3. Determination of QY of CDs by slope method (results: NCDs: 42.2%, N-free CDs: 2.84%).

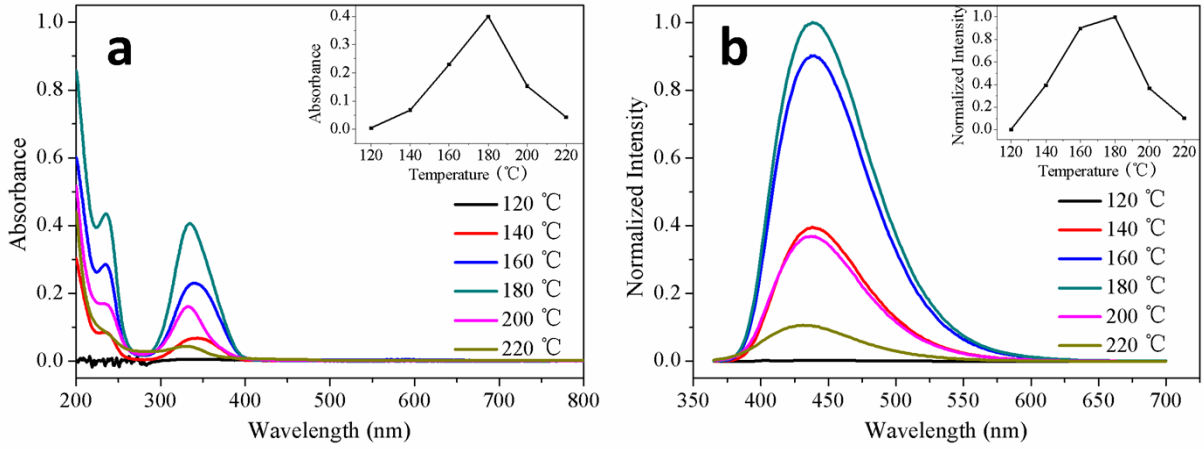

Fig. S4. UV-vis absorption (a) and PL (b) spectra of NCDs aqueous solutions synthesized at different temperature (4.2 g citric acid, 40 mL H_2O, 3.6 g urea, 4 h). The insets are absorbance at 338 nm and fluorescence intensity at 440 nm plotted against temperature, separately (The concentration of NCDs is diluted to 2×10^{-4} times that of the original solution. The excitation and emission slits are both set at 2 nm. λ_{ex}=355 nm).

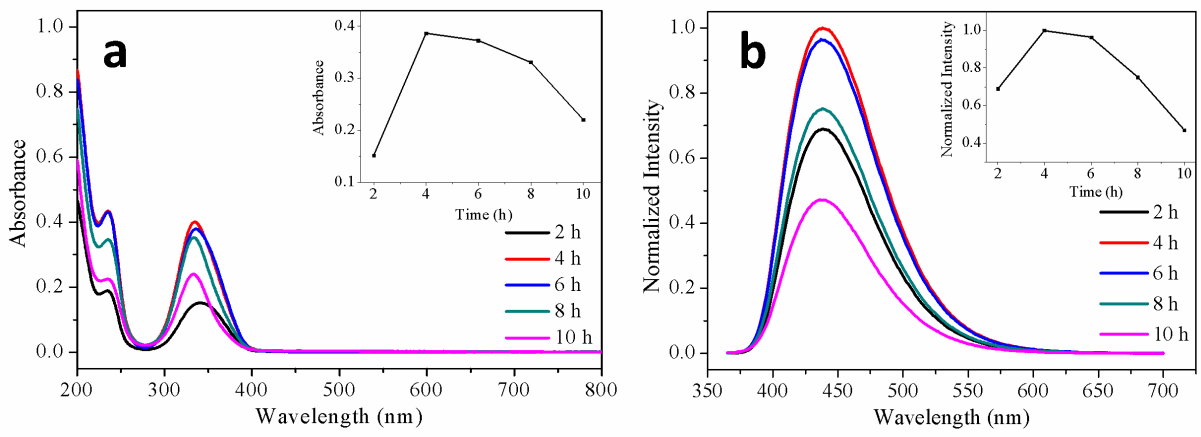

Fig. S5. UV-vis absorption (a) and PL spectra (b) of NCDs aqueous solutions synthesized at different time (4.2 g citric acid, 40 mL H_2O, 3.6 g urea, 180 ℃). The insets are absorbance at 338 nm and fluorescence intensity at 440 nm plotted against time, separately (The concentration of NCDs is 2×10^{-4} times that of the original solution. The excitation and emission slits are both set at 2 nm. λ_{ex}=355 nm).

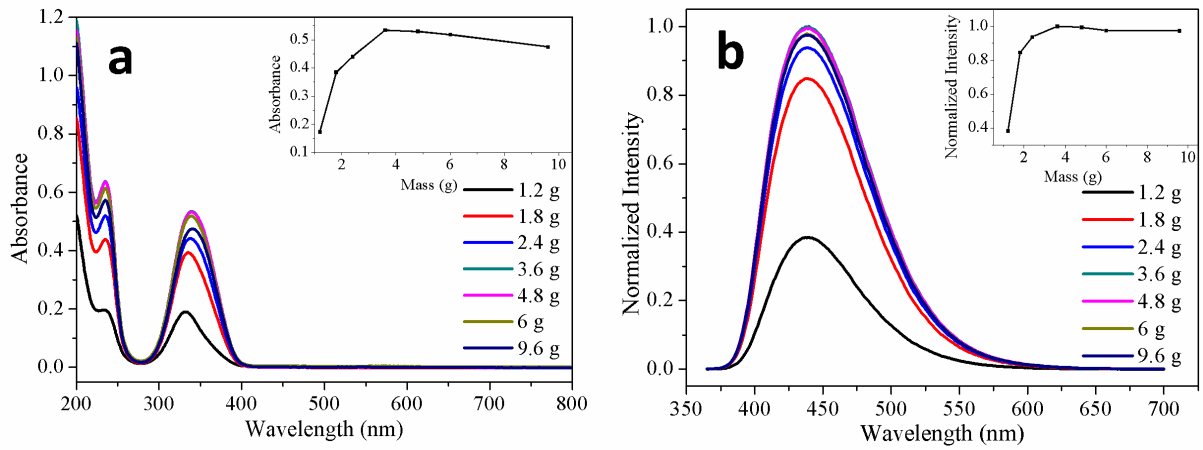

Fig. S6. UV-vis absorption (a) and PL (b) spectra of NCDs aqueous solutions prepared with different mass of urea (4.2 g citric acid, 40 mL H_2O, 180 ℃, 4 h). The insets are absorbance at 338 nm and fluorescence intensity at 440 nm plotted against mass of urea, separately (The concentration of NCDs is 2×10^{-4} times that of the original solution. The excitation and emission slits are both set at 2 nm. λ_{ex}=355 nm).

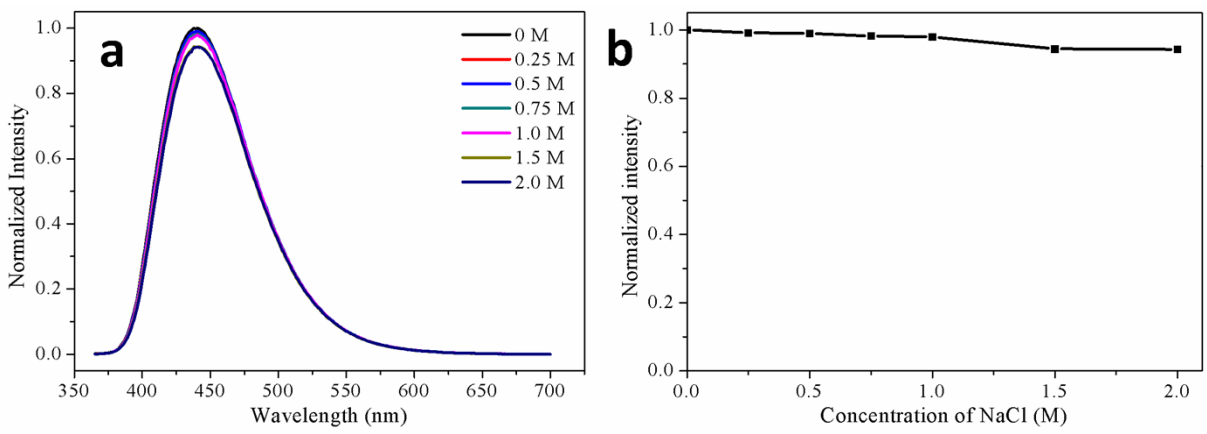

Fig. S7. (a) PL spectra of NCDs aqueous solutions at different concentrations of NaCl (λ_{ex}=355 nm). (b) The relative fluorescence intensity of NCDs aqueous solutions at 440 nm under different concentrations of NaCl solution.

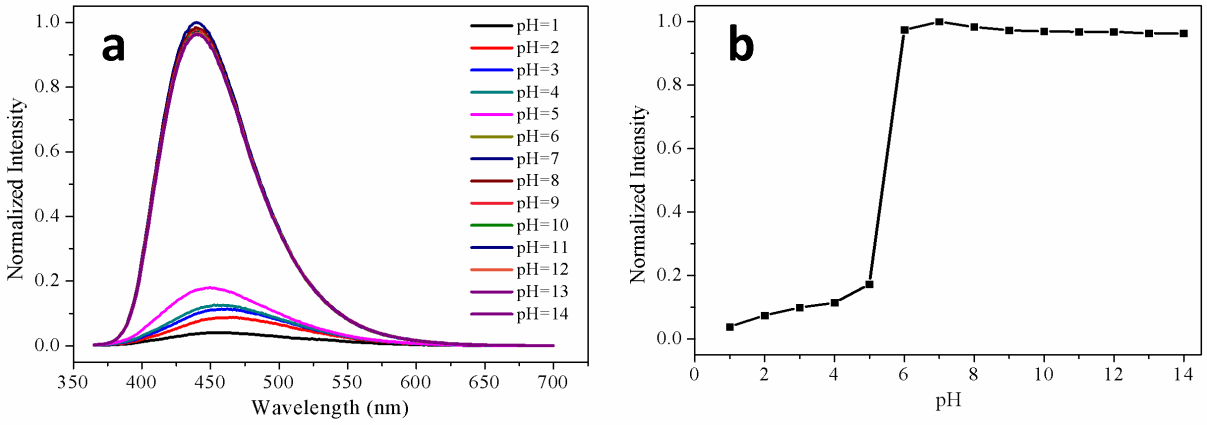

Fig. S8. (a) PL spectra of NCDs aqueous solutions at different pH values (λ_{ex}=355 nm). (b) The relative fluorescence intensity of NCDs aqueous solutions at 440 nm under different pH values.

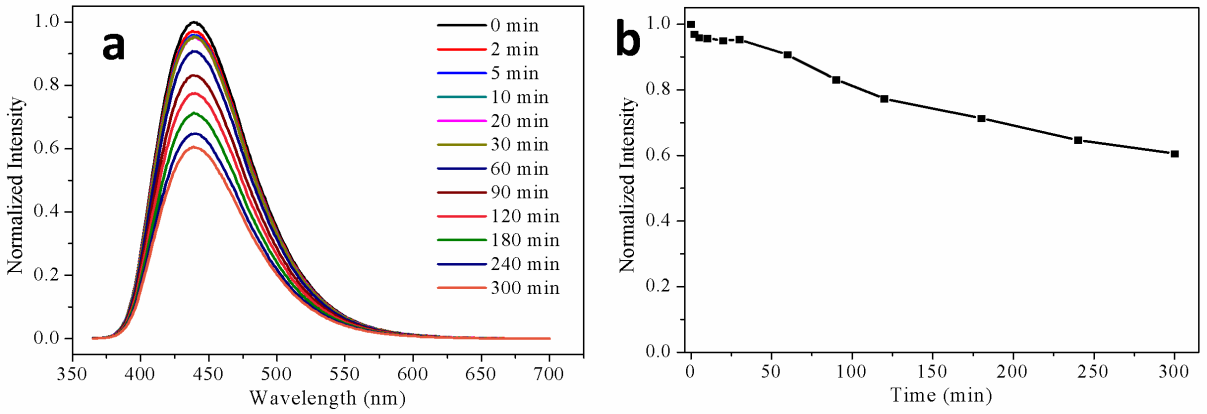

Fig. S9. (a) PL spectra of NCDs aqueous solutions at different time under UV excitation at 365 nm. (b) The relative fluorescence intensity of NCDs aqueous solutions at 440 nm at

different time under UV excitation at 365 nm.

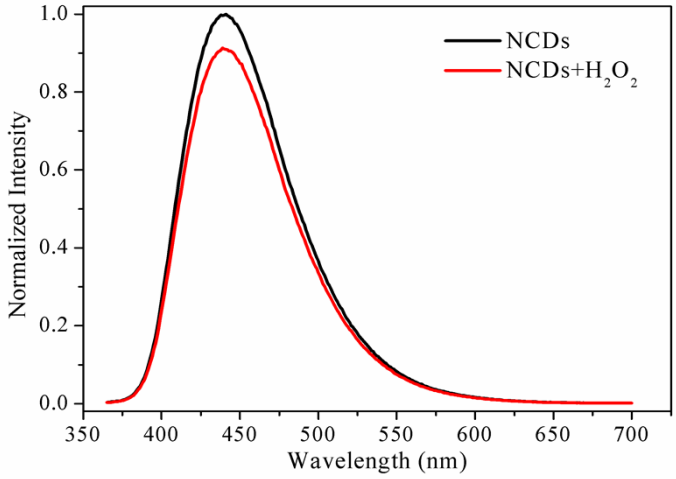

Fig. S10. PL spectra of NCDs aqueous solutions in the absence and presence of 100 mM H_2O_2 (λ_{ex}=355 nm).

Table S1 Comparison of different CDs for Hg^{2+} detection.

Fluorescent probe	Carbon source	LOD (nM)	Linear range (nM)	Ref.
NCDs (hydrothermal)	strawberry	3	10−5×10^4	5
NCDs (hydrothermal)	citric acid	226	10^3−1.2×10^4	7
CDs (Microwave)	flour	0.5	0.5−10	8
CDs (hydrothermal)	pomelo peel	0.23	0.5−10	10
Graphitized CDs (thermal)	ethylene glycol	35	0−10^3	26
NCDs (hydrothermal)	sodium citrate	10	0−5×10^3	27
CDs (thermal pyrolysis)	ethylenediaminetetraacetic acid salts	4.2	0−3×10^3	43
NCDs (hydrothermal)	citric acid	2.91	0−50	This work

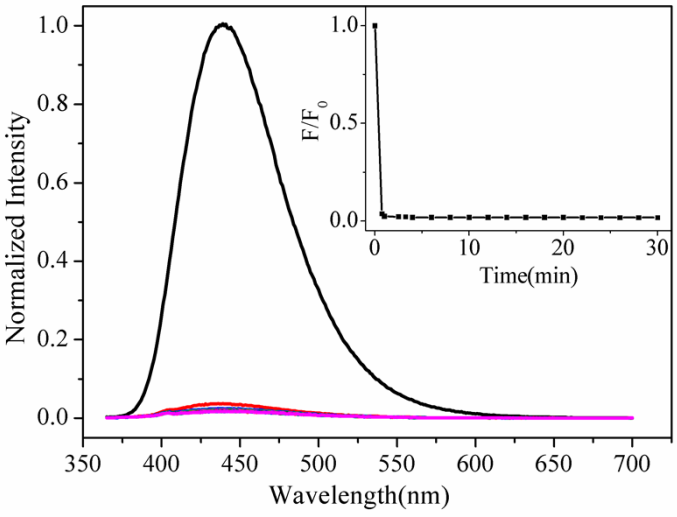

Fig. S11. Time-dependent PL spectra of NCDs-Hg^{2+} dispersion at room temperature. Inset shows the F/F_0 plotted against time in the presence of 40 μM Hg^{2+} (pH 7.0, 0.025 M PBS, λ_{ex}=355 nm, [NCDs]=8 μg·mL^{-1}, [Hg^{2+}]=40 μM; F_0 and F are NCDs aqueous solutions PL intensities at 440 nm in the absence and presence of Hg^{2+}, respectively).

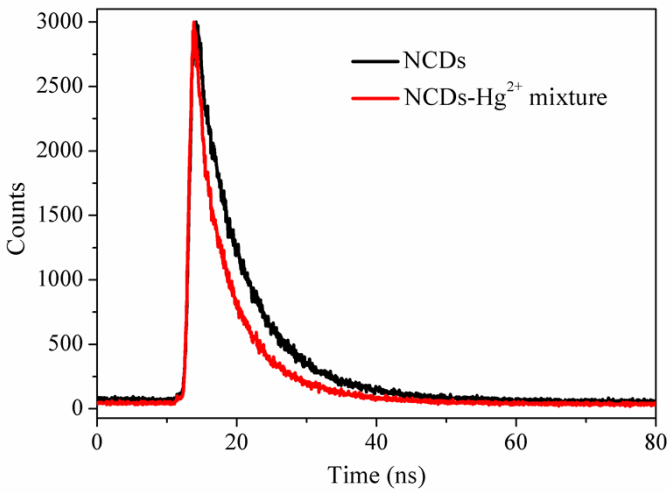

Fig. S12. Fluorescence lifetime decay profiles of NCDs and NCDs-Hg^{2+} mixture with excitations at 375 nm, emission monitored at 450 nm.

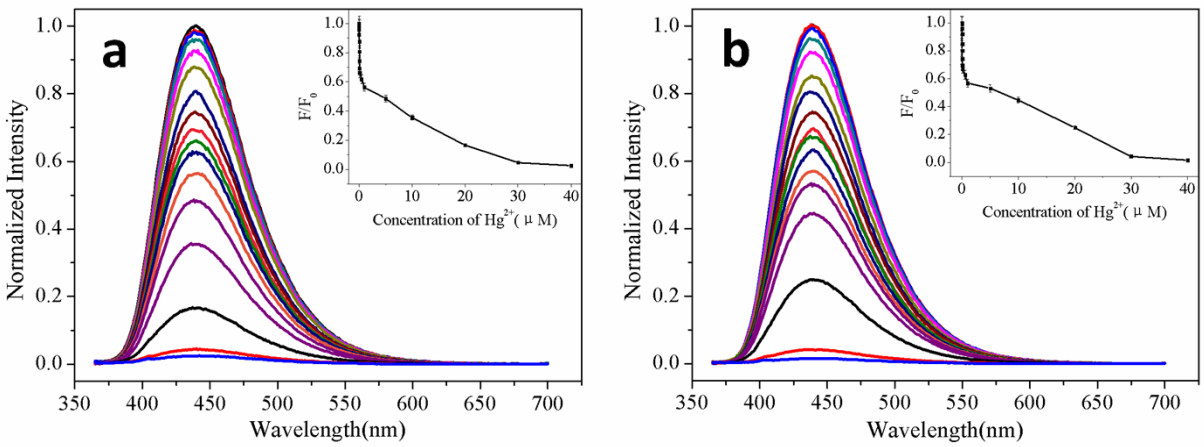

Fig. S13. PL spectra of NCDs in the presence of different Hg^{2+} concentrations (from top to bottom: 0, 0.0005, 0.001, 0.005, 0.01, 0.02, 0.03, 0.04, 0.05, 0.1, 0.5,1, 5,10, 20, 30 and 40 μM) in tap water (a) and commercial bottled mineral water (b). Insets both show the dependence of F/F_0 on the concentrations of Hg^{2+} ions within the range of 0-40 μM. The error bars represent standard deviations based on three independent measurements (pH 7.0, 0.025 M PBS, λ_{ex}=355 nm, [NCDs]=8 μg·mL^{-1}; F_0 and F are NCDs aqueous solutions fluorescence intensities at 440 nm in the absence and presence of Hg^{2+}, respectively).

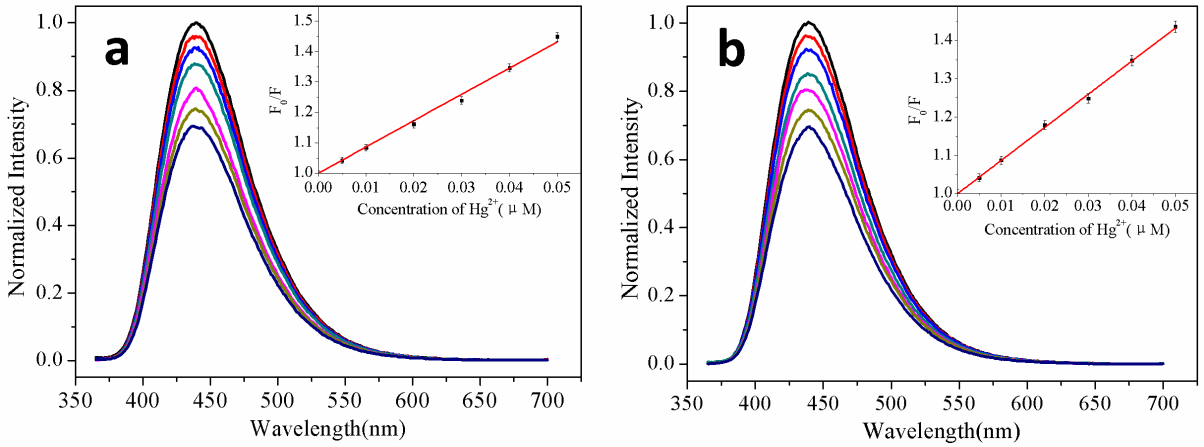

Fig. S14. PL spectra of NCDs in the presence of different Hg^{2+} concentrations (from top to bottom: 0, 0.005, 0.01, 0.02, 0.03, 0.04, 0.05 μM) in tap water (a) and commercial bottled mineral water (b). Insets show the linear relationship of F_0/F versus the concentrations of Hg^{2+} ions over the range of 0-0.05 μM in tap water (a) and commercial bottled mineral water (b), separately. The error bars represent standard deviations based on three independent measurements (pH 7.0, 0.025 M PBS, λ_{ex}=355 nm, [NCDs]=8 μg·mL^{-1}; F_0 and F are NCDs aqueous solutions fluorescence intensities at 440 nm in the absence and presence of Hg^{2+}, respectively).